Study of Strong to Ultratight Protein Interactions Using Differential Scanning Calorimetry†

John F. Brandts* and Lung-Nan Lin

Department of Chemistry, University of Massachusetts, Amherst, Massachusetts 01003

Received November 15, 1989; Revised Manuscript Received April 6, 1990

ABSTRACT: Data from differential scanning calorimetry (DSC) may be used to estimate very large binding constants that cannot be conveniently measured by more conventional equilibrium techniques. Thermodynamic models have been formulated to describe interacting systems that involve either one thermal transition (protein–ligand) or two thermal transitions (protein–protein) and either 1:1 or higher binding stoichiometry. Methods are described for obtaining binding constants and heats of binding by two different methods: calculation or simulation fitting of data. Extensive DSC data on 2′CMP binding to RNase are presented and analyzed by the two methods. It is found that the methods agree when binding sites are completely saturated, but substantial errors arise in the calculation method when site saturation is incomplete and the transition of liganded molecules overlaps that of unliganded molecules. This arises primarily from an inability to determine T_M (i.e., the temperature where concentrations of folded and unfolded protein are equal) under weak-binding conditions. Results from simulation show that the binding constants and heats of binding from the DSC method agree quantitatively with corresponding estimates obtained from equilibrium methods when extrapolated to the same temperature. It was also found from the DSC data that the binding constant decreases with increasing concentration of ligand, which might arise from nonideality effects associated with dimerization of 2′CMP. Simulations show that the DSC method is capable of estimating binding constants for ultratight interactions up to perhaps 10^{40} M^{-1} or higher, while most equilibrium methods fail well below 10^{10} M^{-1}. DSC data from the literature on a number of interacting systems (trypsin–soybean trypsin inhibitor, trypsin–ovomucoid, trypsin–pancreatic trypsin inhibitor, chymotrypsin–subtilisin inhibitor, subtilisin BPN–subtilisin inhibitor, RNase S protein–RNase S peptide, avidin–biotin, ovotransferrin–Fe^{3+}, superoxide dismutase–Zn^{2+}, alkaline phosphatase–Zn^{2+}, and assembly of regulatory and catalytic subunits of aspartate transcarbamoylase) were analyzed by simulation fitting or by calculation. Apparent single-site binding constants ranged from ca. 10^5 to 10^{20} M^{-1}, while the interaction constant for assembly of aspartate transcarbamoylase was estimated as 10^{37} in molarity units. For most of these systems, the DSC interaction constants compared favorably with other literature estimates, for some it did not for reasons unknown, while for still others this represented the first estimate. Simulations show that for proteins having two binding sites for the same ligand within a single cooperative unit, ligand rearrangement will occur spontaneously during a DSC scan as the transition temperature of the unliganded protein is approached. The tendency is to form more of the unliganded and doubly liganded protein than is present at lower temperatures, which then leads to the absence of a transition for the singly liganded form. Although this tendency will always exist, it may not be expressed in systems where the kinetics for ligand rearrangement are slow relative to the experimental scan rate, in which case the ligand distribution will be frozen in the low-temperature configuration and a transition for the singly liganded form(s) might be seen. For the four systems of this type that were examined, only one (ovotransferrin-Fe^{3+}) appeared to remain in a low-temperature configuration during scanning.

Though methods have been described (Schellman, 1975; Crothers, 1971; Marky & Breslauer, 1987) for estimating binding constants from differential scanning calorimetry (DSC) data, these have only occasionally been used to characterize protein–ligand interactions (Schwarz, 1988; Pace & McGrath, 1980) and have never been used to determine interaction constants for protein–protein or other protein–macromolecule reactions. The greatest impediment to this use of DSC is that the method is indirect since the binding constant must be estimated by observing the effect of ligand concentration on the midpoint of the thermal unfolding transition, and this involves model-based assumptions. It has never been demonstrated from careful studies of any protein–ligand system that binding constants obtained from DSC measurements agree quantitatively with those obtained by more direct equilibrium techniques.

Overlooking these problems for the moment, the DSC method does have two important advantages over all equilibrium methods. The first pertains to studies on multidomain proteins, where both a binding domain and a regulatory domain contribute to the ligand-binding process. It was shown in an earlier publication (Brandts et al., 1989) that it is sometimes possible using DSC to obtain the individual free energy contributions of each domain to the binding constant. This can provide important mechanistic information not only for those enzymes that have separate catalytic and regulatory domains (e.g., aspartate transcarbamoylase), but also for the large family of two-substrate enzymes whose active site is sandwiched between the two substrate-binding domains (e.g., phosphoglycerate kinase, hexokinase).

A second major advantage of the DSC method over equi-

† This work was supported by grants GM-11071 and GM-42636 from the National Institutes of Health.

0006-2960/90/0429-6927$02.50/0 © 1990 American Chemical Society

librium methods, not previously emphasized in the literature, appears in the measurement of very large binding constants. To obtain an accurate estimate of binding constant, all direct equilibrium methods require that ca. 10% or more of added ligand remains in the unbound state. As binding constants become larger and larger, working concentrations of protein and ligand must therefore be smaller and smaller and eventually the method fails because the sensitivity of detection is challenged. For reactions of 1:1 stoichiometry, most chemical and optical methods fail in the binding constant range 10^5–10^7 M^{-1} while photon counting of protein fluorescence can sometimes extend the range to 10^{10} M^{-1} (Uehara et al., 1978). In the restricted case where ligand binding totally abolishes enzyme activity (e.g., protease inhibitors), the range has been increased to 10^{12} M^{-1} (Empie & Laskowski, 1982) by observing the inhibition of rapid enzymic turnover of a chromogenic substrate. Finally, by use of radiolabeled pancreatic trypsin inhibitor (BPTI) in competition with weaker inhibitors, a binding constant of 10^{13} M^{-1} was determined for the BPTI–trypsin complex by Vincent and Lazdunski (1972). One of the tightest interaction constants determined for protein–nucleic acid binding is 10^{13} M^{-1} for the *lac* operator–*lac* repressor system (Riggs et al., 1970) by using radiolabeling and filter binding assay. Even beyond this, there are many strongly interacting systems (e.g., assembly of multisubunit proteins and multienzyme complexes, antibody–antigen binding, ribosome assembly, hormone–receptor interactions, etc.) that have not been thermodynamically characterized because suitable methods are lacking.

With the limitations from the concentration–sensitivity cascade inherent in all direct equilibrium techniques, there exists the need for a general method that can be used to study important biochemical interactions that exhibit binding constants from ca. 10^8 to perhaps as high as 10^{50} M^{-1}. Although the DSC method may be justifiably criticized for being indirect, this also provides its major advantage for studying ultratight binding. Not relying on direct observation of the binding equilibria, the DSC method works equally well when ligand is essentially 100% bound, which avoids the necessity of lowering concentrations as interactions become stronger. As will be seen, this provides enormous headroom for measuring very large binding constants, which are inaccessible or difficulty accessible by direct equilibrium methods.

In this paper, appropriate equations will be derived that enable the simulation of DSC curves for interacting species and the calculation of binding constants from experimental data, using the two assumptions that all transitions are two-state in character and ligand binds only to the low-temperature state. This will include treatment of both protein–small ligand (i.e., a single thermal transition) and protein–macromolecule (two transition) systems. Interactions with 1:1 and 2:1 stoichiometry will be discussed, with both independent and interacting sites in the latter case. This treatment will be applied to the very simple reaction involving the 1:1 binding of 2′CMP to the active site of RNase A. It will be shown that the binding constants so obtained agree well with those obtained by direct equilibrium methods when they are extrapolated to identical temperature. Finally, DSC data from the literature will be used to estimate binding constants for some very strong biochemical interactions of both 1:1 and higher stoichiometry and these results will also be compared to literature estimates from equilibrium methods where possible.

Materials and Methods

Bovine RNase (Catalog No. R-5500) and 2′CMP (Catalog No. C7137) were purchased from Sigma Chemical Co. and used without further purification. All other chemicals were of reagent grade.

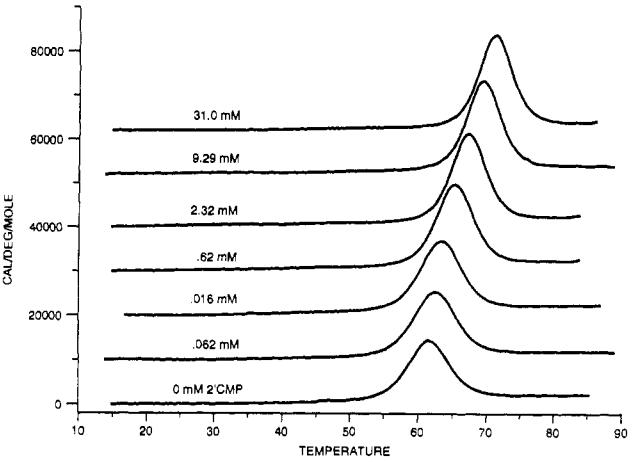

FIGURE 1: Experimental DSC scans on ribonuclease A (0.14 mM) at various concentrations of the inhibitor 2′CMP. Buffer conditions (pH 5.5, 50 mM KOAc, 200 mM KCl) were identical for all samples. Scan rates were 57 °C/h.

Calorimetric measurements were carried out on a MicroCal MC-2 ultrasensitive DSC (MicroCal Inc., Northampton, MA) using the DA-2 software package for data acquisition and analysis. Special software from MicroCal was used for simulation fitting of experimental data. Concentrations of RNase and 2′CMP were determined spectrophotometrically, using molar extinction coefficients of 9800 at 278 nm for RNase and 7400 at 260 nm for 2′CMP at pH 7.0.

During the course of the investigations, it was found that transition midpoints were slightly different from dialyzed and undialyzed samples of RNase, especially at low concentrations of 2′CMP. This presumably occurred because of significant amounts of salt, perhaps phosphates, in the commercial preparation. All of the data presented in this paper were from samples with exhaustive dialysis.

Control studies were carried out on RNase solutions at varying scan rates from 25 to 88 °C/h, both in the presence and in the absence of 2′CMP. Although the T_M values for transitions were shifted higher by ca. 0.2 °C at the highest scan rate, this shift was found to be independent of the amount of ligand in solution so that the same binding constants were obtained, within errors, at the lowest and highest scan rates. It was found that the reversibility of transitions on the second heating was somewhat better at the higher scan rates, however.

Results and Discussion

I. Analysis of the Binding of 2′CMP to RNase A

DSC scans of RNase A (0.14 mM) are shown in Figure I, in the presence of varying concentrations of 2′CMP from 0 to 31 mM. These were obtained in a high-salt buffer (200 mM KCl) at a pH of 5.5 (50 mM KOAc) where the binding of 2′CMP is maximal (Anderson et al., 1968). Similar data were obtained (summarized in Table I) in a low-salt buffer (0 mM KCl, 50 mM KOAc, pH 5.5) over nearly the same concentration range. At these concentrations of protein and ligand, the results are very similar in appearance to simulations from the model (case I) in the Appendix, showing a progressive upward shift in T_M as the ligand concentration increases.

Careful inspection of the DSC scans on RNase, such as those shown in Figure 1, reveals a small problem that has been seen for many other proteins as well. The low-temperature base lines have a slight upward slope while the high-temperature base lines are very nearly flat, which suggests that ΔC_p

Table I: Parameters Obtained from DSC Scans on RNase in the Presence of Varying Concentrations of 2′CMP[a]

2′CMP (mM)	T_M (°C)	$\Delta H_d(T_M)$ (kcal)	ΔC_p (cal/deg)
	0 mM KCl		
0.00	60.85	99.1	1000
0.06	62.41	107.5	830
0.15	63.81	115.9	1050
0.46	65.64	126.7	1230
1.52	67.65	130.7	870
6.09	69.71	131.2	980
15.10	71.04	134.9	1030
36.50	72.11	135.5	1000
	200 mM KCl		
0.00	61.44	105.2	1030
0.06	62.44	112.0	700
0.16	63.30	114.4	870
0.62	65.28	125.8	930
2.32	67.32	128.3	930
9.30	69.51	129.2	950
31.00	71.31	131.8	840

[a] The RNase concentrations were ca. 0.14 mM, and the buffer was 50 mM KOAc, pH 5.5.

is strongly temperature-dependent and should change sign somewhere in the experimental range of T_M values. This does not happen, however, since there was no indication that the average ΔC_p value was dependent on T_M. No suitable explanation has been given as yet for this behavior. We have worked around this problem by linearly extrapolating each base line to T_M and taking the ΔC_p at that point. These values are shown in Table I. The area progression curve between the two base lines was obtained by an appropriate algorithm and this was then subtracted from the experimental curve in order to remove the ΔC_p effect and coincide the low- and high-temperature base lines. The area (ΔH_d in Table I) was then obtained by trapezoidal integration. The temperature where the total area is divided into two equal portions is designated as T_M.

A plot of ΔH_d at T_M minus ΔH_d at T_0 (T_0 is the midpoint at zero ligand concentration) versus T_M minus T_0 is shown in Figure 2 for data in both the low-salt and high-salt buffers. In each case, ΔH_d increases rapidly at low ligand concentration (i.e., small $T_M - T_0$), reflecting low-temperature saturation of sites having a negative heat of binding, which then adds to the transition heat when the ligands are relased upon unfolding. Once saturation is completed, the curves rise more gradually and reflect only the increase in ΔH_d arising from the positive ΔC_p of unfolding. The solid lines represent the ideal calculated curves (eq 10 in Appendix), which assume a $\Delta H_d(T_0)$ of 99 kcal (low salt) and 105 kcal (high salt), heat of binding ΔH_L of −25 kcal (low salt) and −17 kcal (high salt), a ΔC_p of unfolding of 1000 cal/deg·mol for both cases, and best values of binding constants (discussed below). The average deviation of fit is ca. 2 kcal, which is within calorimetric errors.

Binding constants from the data in Table I may be estimated in either of two ways as outlined in the Appendix: (1) By use of the estimates of T_0, ΔH_d at T_0, and ΔC_p in the absence of ligand, curves may be simulated (case I model) using various values of ΔH_L and $K_L(T_0)$ until the simulated curve at appropriate concentration of protein (P_t) and ligand (L_t) agrees well with the experimental curve in terms of T_M and $\Delta H_d(T_M)$. (2) By use of the estimates of T_0, T_M, ΔH_d at T_0, and ΔC_p, the value of K_L may be calculated directly from eq 6 in the Appendix. Both of these methods provide an estimate of $K_L(T_0)$ for each of the scans in Figure 1 except the zero-ligand control. What was found was that the two methods agree well only when the ligand concentration is 5-fold higher, or more, than the protein concentration. At lower ligand concentrations,

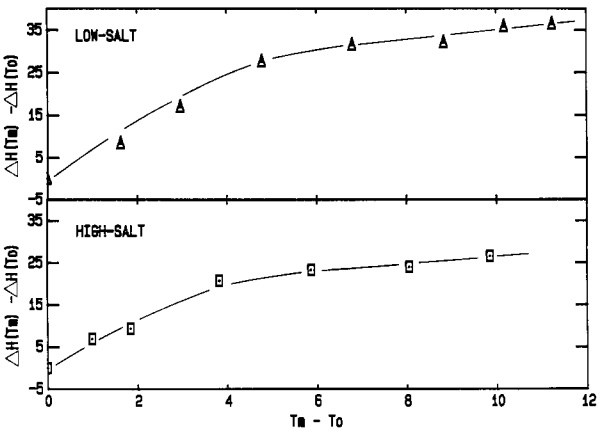

FIGURE 2: Change in the heat of transition (kilocalories per mole) as a function of the transition midpoints, both relative to the same variables in the absence of 2′CMP. The upper panel is for data in the low-salt buffer (0 mM KCl) and the bottom panel for data in the high-salt buffer (200 mM KCl). The solid lines are calculated curves (see text).

the estimates from method 2 are inaccurate by as much as 100%. Simulations show that this is due to an inability to determine the appropriate T_M for use in eq 6. At low ligand-to-protein ratios, the shape of the transition curve becomes distorted (i.e., ΔH_{vH} is less than ΔH_{cal} and the transition peak is skewed to the high-temperature side) even when the heat of binding is zero. More importantly for systems such as ours with a large heat of binding, the temperature where half of the heat effect occurs is no longer the point where the concentrations of folded and unfolded molecules are equal as required by eq 6. This problem develops because molecules that unfold in the low-temperature portion of the transition are largely unliganded while those unfolding in the high-temperature portion are largely liganded, as will be shown later in more detail, so that area generated under the curve does not bear a constant proportionality to number of unfolded molecules throughout the entire transition range.[1] Using the temperature of 50% area completion for T_M in eq 6 will overestimate the value of K_L when the heat of binding is negative and will underestimate it when the heat of binding is positive. This is not a problem at high ligand concentrations, where proportionality will be maintained if all molecules that participate in the transition are liganded. This point has been overlooked in previous treatments of ligand binding (Schellman 1975; Crothers 1971), all of which relied on equations similar to eq 6.

The estimates of $K_L(T_0)$ as a function of [2′CMP] obtained by method 1 are shown in the log–log plot of Figure 3 for both the low-salt and high-salt buffers. It is seen that the apparent value of K_L becomes smaller as [2′CMP] increases above concentrations of ca. 1 mM, and this effect is stronger in the

[1] There is another problem, similar to the one described here but smaller in magnitude, which can sometimes make it difficult to locate the exact T_M for a transition. If the ΔC_p for a transition is positive, as is usually the case, then molecules unfolding in the low-temperature portion of a transition do so with a smaller ΔH than those unfolding in the high-temperature portion of the transition so there is not a constant proportionality between the area generated and the number of unfolded molecules. Although the treatment of data used here eliminates the effect of ΔC_p on the base line, it does not eliminate its effect on ΔH so this problem persists even after data reduction. The error in calculated K_L introduced from this will usually be negligible at ligand concentrations where T_M is more than several degrees higher than T_0. It will introduce no error into the K_L obtained from simulations at any concentrations, since this effect will be included in both the simulated data and experimental data.

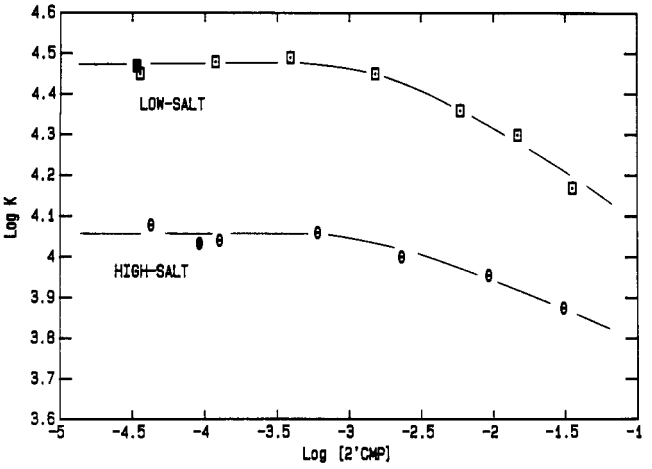

FIGURE 3: Variations in the apparent binding constant K_L as a function of the concentration of free inhibitor [2'CMP]. The empty symbols are data obtained from these DSC studies at 61 °C, while the filled symbols are data obtained from titration calorimetry at a lower temperature and extrapolated to 61 °C.

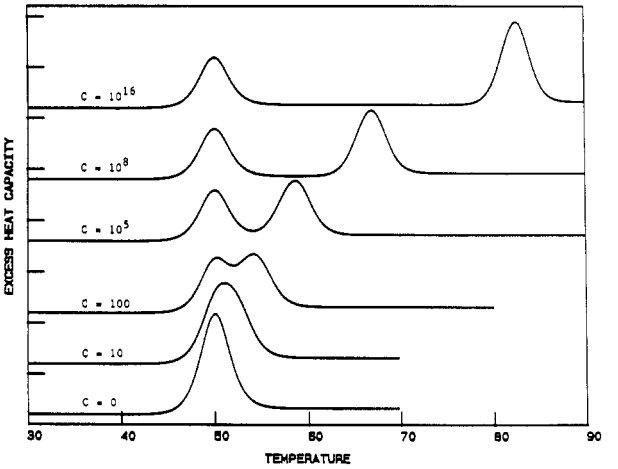

FIGURE 4: Simulations of DSC curves when the total ligand concentration is half of the protein concentration. The protein has assumed transition parameters of 50 °C for T_0, 200 kcal for $\Delta H(T_0)$, and 3000 cal/deg for ΔC_p. The C parameter measures the tightness of binding and is equal to the product of the protein concentration times the binding constant at T_0. The heat of binding was assumed to be −10 kcal and temperature-independent.

low-salt case where the binding constant is larger. These deviations at high concentration are real, we feel, since simulations show they go beyond any reasonable errors in DSC parameters. There are at least two possible explanations. First, the model used to analyze the data assumes that 2'CMP *cannot* bind to denatured RNase. However, if it were to bind weakly to the unfolded form, then the apparent binding constant $K_L(T_0)$ would decrease at high 2'CMP concentrations where this becomes significant. Second, the decrease in apparent $K_L(T_0)$ values might also be caused by concentration-dependent decreases in the activity coefficient of 2'CMP. It is known that solutes similar to 2'CMP show a strong tendency to dimerize at high concentrations (Ts'o et al., 1969) so that we favor the second explanation based on nonideality, but it is possible other factors are involved as well.

The limiting value of $K_L(T_0)$ at low [2'CMP] is 31 000 M^{-1} in the low-salt buffer and 11 500 M^{-1} in the high-salt buffer, with indicated heats of binding ΔH_L of −25 000 and −17 000 cal/mol, respectively. Precise binding constants for the 2'CMP/RNase system have previously been obtained by an equilibrium method (i.e., titration calorimetry) in these same two buffers [Wiseman et al. (1989); Unpublished observations from this laboratory] at lower temperatures. In the low-salt buffer at similar RNase concentration, the values obtained for K_L, ΔH_L, and ΔC_{pL} at 28 °C (900 000 M^{-1}, −17 700 cal/mol, and −180 cal/mol·deg) may be extrapolated to 61 °C (i.e., T_0), leading to a K_L value of 29 600 M^{-1} and a ΔH_L value of −23 700 cal/mol. Both of these parameters agree nicely with the corresponding DSC estimates (31 000 M^{-1} and −25 000 cal/mol) at the same temperature. In the high-salt buffer, the parameters from the equilibrium method at 28 °C (115 000 M^{-1}, −12 200 cal/mol, and −130 cal/deg·mol) extrapolate to a K_L of 10 800 M^{-1} and a ΔH_L of −16 500 at 61 °C, which are again very close to the estimates from the DSC method (11 500 M^{-1} and −17 000 cal/mol). These extrapolated estimates for K_L are shown as the solid symbols in Figure 3. Equilibrium methods are not well-suited for detecting effects introduced from nonideality of the ligand (since all measurements must be made at a free ligand concentration very close to the value of the reciprocal binding constant) so that interesting aspect of the DSC data cannot be corroborated.

As mentioned above, distortions in the shape of the transition curve may occur when the ligand concentration is small relative to the concentration of binding sites on the protein. This effect has been observed by DSC earlier for the binding of hydrophobic ligands to defatted human serum albumin (Shrake et al., 1984; Ross & Shrake, 1988; Shrake & Ross, 1988), where it was observed that addition of ligands of high affinity can result in the presence of two transitions associated with ligand-poor and ligand-rich molecules of serum albumin. These effects have been simulated thermodynamically by Shrake and Ross (1990) and by Robert et al. (1988).

Our treatment (case I in the Appendix) for 1:1 stoichiometry differs from those cited above and includes not only ΔC_p effects associated with the transition but also ΔH and ΔC_p effects associated with binding. It also allows calculation of equilibrium concentration of each species at any temperature. Simulations show that distortion of the transition is maximal when the ligand concentration is half the concentration of binding sites (i.e., $L_t/P_t = 0.5$ for 1:1 stoichiometry) and that if this ratio is fixed, as well as all transition parameters, then the shape of the transition curve depends not on the binding constant itself but on the product of the binding constant times the concentration of sites, a unitless parameter we will call C [see Wiseman et al. (1989)].

Some simulations at various C values and L_t/P_t of 0.5 are shown in Figure 4, for a transition with T_0 of 50 °C, $\Delta H(T_0)$ of 200 kcal, and ΔC_p of 3000 cal/deg. The heat of binding was assumed to be −10 kcal and temperature-independent. For this sytem, distortions are already obvious at a C value of 10 as the transition curve has become broadened relative to the situation in the absence of ligand ($C = 0$). As C is increased further, the DSC simulations begin to show two overlapping transitions ($C = 100$), which become completely separated at higher C since the first transition remains at T_0 and the second shifts to progressively higher T_M. Assuming that the DSC measurements are made at P_t of 0.1 mM, then the final scan ($C = 10^{16}$) with a T_M of 82.7 °C corresponds to a binding constant of 10^{20} M^{-1}. Even for a binding constant of 10^{40} M^{-1}, a peak could still be seen within the accessible temperature limit of 120 °C for ultrasensitive DSC.

This separation into two transitions when the ligand is in short supply, seen in Figure 4, does not depend on having slow rate constants for ligand dissociation since, as T_0 is approached and exceeded, it is thermodynamically more favorable for the ligand to provide total stabilization to a few molecules rather than partial stabilization to all. This is true even though, below

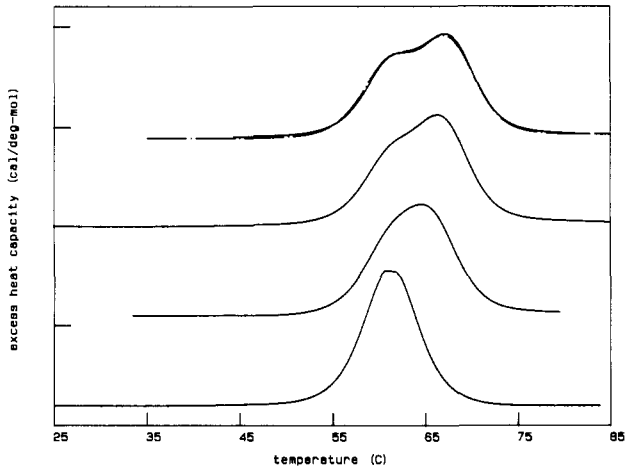

FIGURE 5: Experimental scans on RNase at high concentrations. The lower scan is a control at 3.84 mM RNase in the absence of 2′CMP. The other three scans at 0.56, 1.48, and 2.88 mM RNase (in order, from bottom to top) each contained 2′CMP at half the molar concentration of the RNase. For the top scan with 2.88 mM RNase, the dashed curve shows the simulated fit assuming a binding constant of 20000 M^{-1} and a heat of binding of −29 kcal. In all cases, the buffer was 50 mM KOAc (pH 5.5) and no added KCl.

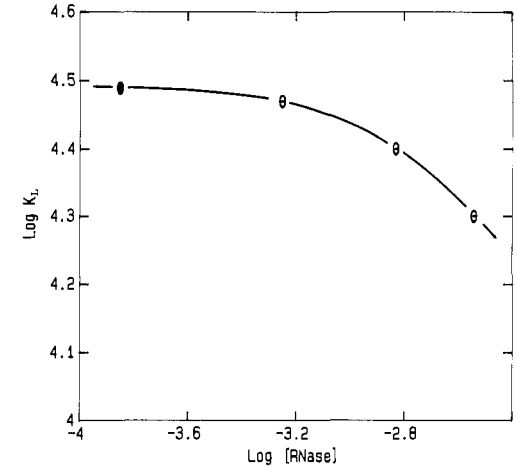

FIGURE 6: Binding constants obtained from simulation fitting of the data in Figure 5 at 0.56, 1.48, and 2.88 mM RNase (open circles). The filled circle is the binding constant obtained from the data in Table I at 0.14 mM RNase.

T_0, the ligand may interact equally with all molecules over a very short time span.

Although this method can be used to estimate very large binding constants, as suggested above, we will apply it here to the RNase/2′CMP system where the binding constant is reasonably small. Because it is small, it was necessary to go to high RNase concentration in order to make the C value large enough (cf. Figure 4) to produce significant distortions in the transition. Experimental scans are shown in Figure 5 at three high concentrations from 0.56 to 2.88 mM in the low-salt buffer, as compared to 0.14 mM used for the scans in Figure 1. For all of these, the L_t/P_t ratio was 0.5, and as predicted, the distortion is more significant at higher protein concentrations. A control experiment without ligand at 3.84 mM RNase is also shown in Figure 5, and it was ascertained in other scans (not shown) that the parameters for the transition in the absence of ligand [T_0 = 61.2, $\Delta H(T_0)$ = 108 kcal, ΔC_p = 300 cal/deg] are reasonably constant over the range 1–4 mM, even though slightly different than at very low concentration (Table I).

With the intrinsic parameters given above, each of the three transitions in Figure 5 was subjected to simulation fitting, using $\Delta H_L(T_0)$ and $\Delta K_L(T_0)$ as fitting parameters with ΔC_{pL} set equal to zero. All could be fit quite well with the same ΔH_L of −29 kcal while the K_L values ranged from 29500 (0.56 mM) to 25000 (1.48 mM) to 20000 M^{-1} (2.88 mM). The fit curve for the 2.88 mM case is shown in Figure 5. All of these K_L values are plotted in Figure 6 as a function of RNase concentration. Also, the earlier limiting K_L value obtained at 0.14 mM RNase is plotted as the filled symbol. That all points lie on nearly the same line shows that the two methods of estimation (i.e., from shape changes at high protein and low ligand concentrations and from T_M changes at low protein and high ligand concentrations) give similar results. The fact that the estimated K_L values decrease with increasing RNase concentration is expected, since this was established earlier with an equilibrium method (Wiseman et al., 1989). It was suggested this might be due to dimerization of RNase to a form that binds 2′CMP less strongly than monomer. Although this may be correct, it is also possible that the decrease in apparent binding constant with increasing concentration might be due to nonideality effects associated with 2′CMP rather than with RNase, since its bulk concentration is increasing at the same rate as for RNase in the data of Figure 6. In this way, the concentration effects seen in Figure 6 and in Figure 3 might be explained by the same factor.[2]

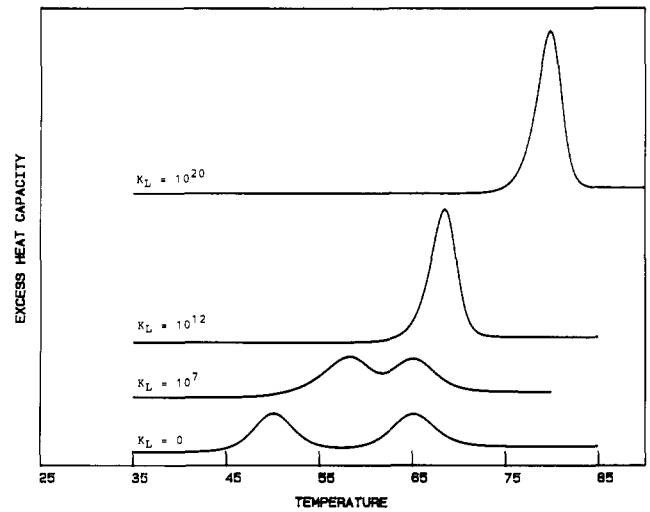

FIGURE 7: Simulated DSC curves for two molecules, both of which undergo a two-state thermal unfolding transition. Both transitions were assumed to have $\Delta H(T_0)$ of 150 kcal and ΔC_p of 2000 cal/deg, while the T_0 values are 50 °C for the least stable and 65 °C for the most stable of the two. The assumed values of the interaction constant (M^{-1}) at 50 °C are listed for each scan, and the heat of interaction was −20 kcal in all cases.

II. Simulations for Protein–Protein Interactions of 1:1 Stoichiometry

When interactions between two protein molecules are studied by DSC, the situation becomes more complicated (case II in the Appendix) since there will be two unfolding transi-

[2] It was incorrectly assumed in the earlier publication from this laboratory (Wiseman et al., 1989) that the decrease in apparent binding constant with increasing concentrations of 2′CMP and RNase could be due to aggregation effects from the protein but not from ligand. In fact, those results from titration calorimetry as well as these from DSC shown in Figure 6 could result from nonideality effects associated with either participant in the binding reaction. However, the DSC results shown in Figure 3, if they arise from nonideality effects, are more likely associated with the ligand since the RNase concentration was held constant and only the concentration of 2′CMP was varied, in contrast to the situation in Figure 6 where both concentrations changed.

tions. For simulation purposes, it will be assumed that each transition has a ΔH of 150 kcal at its intrinsic midpoint, ΔC_p of 2000 cal/deg, and intrinsic midpoints T_0 of 50 and 65 °C. If it is further assumed that the concentration of each is 0.1 mM and that the heat of interaction is −20 kcal and independent of temperature, then simulations may be carried out for different values of the interaction constant $K_L(T_0)$ and these are shown in Figure 7. The bottom simulated scan is for the noninteracting system, $K_L = 0$, which shows the reference transitions at the intrinsic midpoints of 50 and 65 °C in the 1:1 mixture. For a reasonably small interaction constant ($K_L = 10^7$ M^{-1} in the second scan), the transition of the 1:1 complex is seen at ca. 58 °C. Since this is below the intrinsic midpoint for the more stable component, the melting of the complex produces one folded and one unfolded molecule so that unfolding of the second component is still seen at 65 °C. However, when the interaction constant is 10^{12} M^{-1}, the T_M of the complex is higher than both intrinsic T_0's and only a single transition is seen at 68 °C. Because of cooperativity introduced by the strong interaction between the two, this occurs as a single two-state transition. In situations where the starting concentrations are not in the same ratio as the stoichiometry of the complex, then an additional transition would also be seen at the intrinsic midpoint of the component that is in excess. The final simulated scan in Figure 7 pertains to a stronger interaction constant of 10^{20} M^{-1}, where the corresponding midpoint is 80 °C.

Experimental data on interacting proteins (or on other protein–macromolecule interactions) may be analyzed either by simulation or by calculation, as outlined in the Appendix, to obtain binding constants and also heats of binding if the DSC data are sufficiently accurate. When available, it is better to use more accurate heats and heat capacities of binding that have been obtained independently from mixing calorimetry. These may then be treated as known parameters along with the intrinsic DSC parameters for both transitions (i.e., the heat and heat capacity of transition 1 at T_0, the heat and heat capacity of transition 2 at T_0') and T_M for the complex so that analysis by simulation or calculation focuses on only one unknown parameter, K_L at T_0.

Although all of the derivations in the Appendix are based on the assumption of two-state transitions, it seems likely that this criterion may often be relaxed without encountering serious errors in estimates of interaction parameters. The derived results are formally insensitive to the precise mechanism of unfolding but require only that the ΔH for the transition(s) that is used in the simulations (or calculations) represents the true difference in enthalpy of initial and final states, that the T_M and T_0 represent in the intended way the relative free energy of initial and final states (i.e., irrespective of any intermediates that might also exist), and that the low-temperature state is the only form that binds ligand. For those transitions that are not two-state, it is therefore better to use the calorimetric ΔH, rather than van't Hoff, and to carry out simulations for the purpose of reproducing only the midpoint and total calorimetric heats of transitions but not their van't Hoff ΔH.

III. Simulations for Protein–Ligand Binding at 2:1 Stoichiometry

These simulations pertain to case III in the Appendix for a protein that has a single cooperative unfolding unit but has two different sites (either identical or nonidentical) with intrinsic binding constants K_{L1} and K_{L2} for the same ligand L. The first ligand bound to a protein molecule will do so according to the appropriate intrinsic binding constant, while

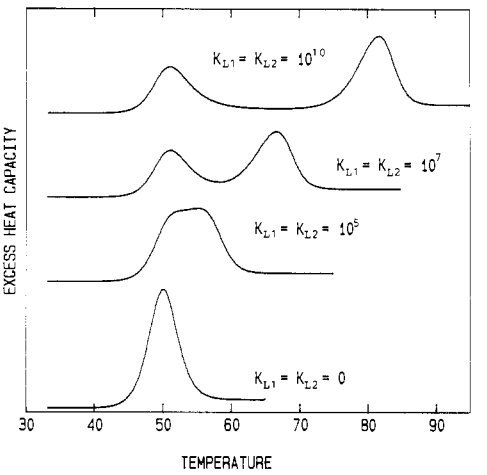

FIGURE 8: Simulated DSC curves for a single-transition protein that has two sites for binding a small ligand. The concentrations of protein and ligand were each assumed to be 0.1 mM so that only half of the sites could be saturated. The bottom scan is the noninteracting control where both binding constants are zero, while the top three scans show a progressive separation of the protein transition into two peaks as the interaction constants become larger. The transition at lower temperature is for protein that has no attached ligand, while that at higher temperature is for protein with two attached ligands.

the second will do so according to the binding constants kK_{L1} or kK_{L2} as is appropriate. The k factor incorporates the possibility of site–site interactions and is equal to $\exp(-\Delta G_{12}/RT)$, where ΔG_{12} is the additional free energy conferred to the doubly liganded species relative to the sum of the two singly liganded species. If k is unity, the two sites are independent, while the sites will saturate cooperatively for values larger than unity and with negative cooperativity for values less than unity.

Simulations are shown in Figure 8 for a protein with T_0 of 50 °C, ΔH at T_0 of 150 kcal, and ΔC_p of 2000 cal/deg·mol. For this illustration the sites are assumed identical ($K_{L1} = K_{L2}$; $\Delta H_{L1} = \Delta H_{L2} = -10$ kcal) and independent ($k = 1$). To illustrate an important point, the protein and ligand concentrations are identical ($N_t = L_t = 0.1$ mM) so that the system will have only half of the sites saturated on average. These simulations show that only one transition is seen in addition to that for the unliganded protein at T_0. This corresponds to melting of the double liganded species. As the K_L values are increased, the midpoint for melting of this double liganded complex shifts to higher temperatures, as seen.

At first glance, it is surprising that no transition is seen for the melting of the singly liganded species since simple statistics suggest that at a 1:1 ratio of protein to ligand for two independent, identical sites, there should be twice as many singly liganded molecules as doubly liganded. This is true in fact at temperatures below T_0, as illustrated in Figure 9A. Using the same parameters as in the last scan of Figure 8, a plot is shown for the fraction of both the singly and doubly liganded species as a function of temperature along with the corresponding DSC curve. As the intrinsic T_0 is approached and exceeded, there is a rearrangement of attached ligand that acts to increase the population of the doubly liganded species at the expense of the singly liganded form. This is favorable thermodynamically since, above T_0, free energy must be expended in order to prevent the unfolding of the protein so that it becomes advantageous to "protect" as few protein molecules as possible consistent with 100% ligand binding. Simulations show that this rearrangement occurs for all systems of this type so long as K_{L1} and K_{L2} are of similar magnitude. Thus, sites that are independent below T_0 become cooperative above T_0

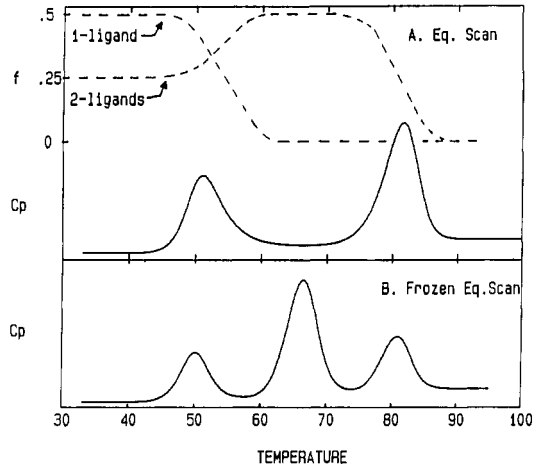

FIGURE 9: Equilibrium scan and frozen equilibrium scan for the system shown in the top scan of Figure 8. (A) When equilibrium is reestablished at each temperature along the scan axis, the low-temperature distribution of ligand (i.e., 25% of the protein is unliganded, 50% has one attached ligand, and 25% has two attached ligands) changes abruptly as the scan temperature approaches and exceeds the transition temperature of the unliganded protein, as seen in the dashed curves at the top, which show the fraction f of the one- and two-liganded species. Because of this redistribution of ligand near T_0, no transition is seen for the single-liganded species. (B) This shows the scan that would result for the same system if no redistribution of ligands takes place during the scan. In this case, 25% of the protein unfolds in the unliganded form, 50% in the single-ligand form, and 25% in the double-ligand form.

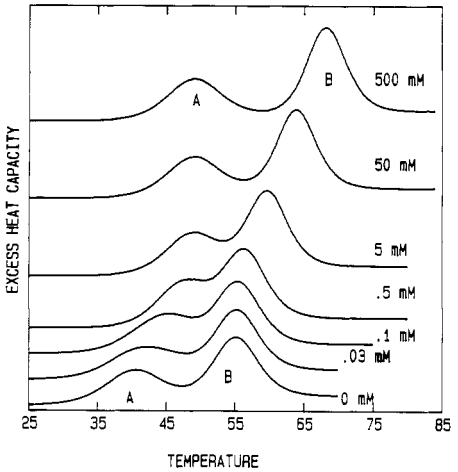

FIGURE 10: Simulated scans for a protein with two interacting domains A and B, whose interactions become stronger when the ligand binds to the binding domain B. At low ligand concentration below 5 mM, only the transition for the A domain is affected as it shifts from 40 °C (i.e., T_{0A}) to ca. 50 °C while the B transition is unaffected and remains at 55 °C (T_{0B}). At ligand concentrations above 5 mM, the effect on the A transition saturates and further increases in ligand concentration shift only the B transition. This effect does not saturate since the B transition continues to shift with the logarithm of the ligand concentration up to the highest concentrations possible. Other parameters used for the simulations were $\Delta H_A(T_{0A})$ of 70 kcal, $\Delta H_B(T_{0B})$ of 100 kcal, ΔC_p of 2000 cal/deg for each transition, K_L(50 °C) of 4000 M^{-1}, ΔH_L of −10 kcal, k of 25, and a protein concentration of 0.1 mM.

since they are mutually coupled to the unfolding transition and therefore to each other.

Whenever one of the binding constants exceeds the other by several orders of magnitude, a separate transition may be seen for the singly liganded form since the difference in intrinsic binding free energy is sufficient to counteract ligand rearrangement above T_0. Likewise, in the case of identical sites with negative cooperativity, a separate transition will also be seen for the singly liganded form when k is smaller than ca. 0.001. Even in these cases, however, the size of this transition will be smaller than predicted from ligand distribution below T_0.

It is commonly observed for tight-binding systems that exchange between bound and free ligand can take as long as hours, days, or even weeks at room temperature and below [e.g., a half-time of 1.04 years at 4 °C has been reported by Garlick and Giese (1988) for the dissociation of a radiolabeled biotin derivative from avidin]. On the other hand, it may require only a few minutes of scan time to pass through the critical temperature region where ligand rearrangement must take place to produce the DSC pattern shown in Figure 9A. There may be instances then when the ligand distribution among sites will be completely or partially frozen in the low-temperature configuration, as will be shown later to possibly occur for the binding of Fe^{3+} to ovotransferrin when examined with a very fast DSC scan rate. For a completely frozen equilibrium, the scan depicted in Figure 9B rather than that in A would be observed and this shows separate transitions for the singly and doubly liganded protein. In principle, it is possible to obtain more information under frozen equilibrium conditions since separate estimates of K_{L1}, K_{L2}, and k might be available whereas under equilibrium conditions only the product $kK_{L1}K_{L2}$ can be estimated and all information regarding cooperativity and nonidentity of sites is lost. It seems unlikely that this will occur often when slow scan rates are used since exchange rates will increase dramatically near transition temperatures where exchange from the unfolded form becomes possible.

IV. Binding of Ligand to a Protein with Two Interacting Domains

Although this particular system was considered earlier (Brandts et al., 1989) in a paper dealing with interacting protein domains, only the analysis of data by calculations was presented. At the time, we were unaware of the problems that can arise from the calculation method whenever T_M is close to T_0 (which is often the case for two-domain systems). In such instances, the simulation method for extracting binding parameters is preferred, for the reasons discussed earlier, and will be presented briefly here (see case V in the Appendix).

For these systems, it will be assumed that the ligand L attaches directly to the more stable B domain of intrinsic midpoint T_{0B} but that its interaction with the B domain is influenced by ligand-dependent changes in interactions between the binding domain B and the regulatory domain A (with intrinsic midpoint T_{0A}). It is further assumed that all interactions between the two domains vanish as soon as either domain unfolds. The binding constant of L to B is K_L when the A domain is unfolded and is kK_L [K^0_L in the terminology of Brandts et al. (1989)] when the A domain is folded. The enhancement parameter k is then equal to $\exp[-\Delta(\Delta G_{AB})/RT]$, where $\Delta(\Delta G_{AB})$ is the difference in interaction between native A and B domains in the presence and absence of site saturation.

Simulations for this system are shown in Figure 10 with assumed parameters as given in the legend. The fact that k is 25 means that ligand binding increases the favorable interactions between A and B so that binding to the native form will be 25 times stronger than binding to the form where the regulatory A domain is unfolded but the binding domain B is intact. As seen in Figure 10, this situation leads to a shift upward in T_M for the A transition at low ligand concentration until a concentration of ca. $1/K_L$ is reached whereupon the

effect on the A transition saturates and further increases in the concentration of ligand cause the B transition to shift higher. Some two-domain proteins known to exhibit the effect simulated here are phosphoglycerate kinase (with one of its substrates, MgATP) and creatine kinase (with one of its substrates, MgADP) which were discussed earlier (Brandts et al., 1989). It seems likely that other such two-domain, two-substrate enzymes, which contain the active site at the interdomain cleft, might also show this behavior when examined carefully by DSC.

V. Analysis of Literature DSC Data on Strongly Interacting Systems

In this section, existing DSC data on a number of tight-binding systems will be discussed. Binding parameters will be estimated and compared with literature values obtained by other methods where possible. It should be emphasized that literature values from different laboratories are sometimes in serious disagreement, particularly for the tightest interactions, and we have generally followed the expeditious practice of choosing the most recent estimate for comparison. For most of the systems to be discussed, heats and heat capacities of binding are also available from mixing calorimetry [see Hinz (1983)] and these were incorporated as fixed parameters in the DSC simulations in order to find the best values for the binding constant. Although the binding constants reported below are mostly from the simulation method, these agree well with those from the calculation method in all cases since the large binding constants avoided the problems that arise from overlap of the transitions of liganded and unliganded protein.

Binding of S Peptide to RNase S Protein. Careful DSC studies have been carried out in Sturtevant's laboratory (Tsong et al., 1970; Hearn et al., 1971) on both RNase S protein [T_0 of 35 °C, $\Delta H(T_0)$ of 55 kcal, ΔC_p of 1400 cal/deg] and its complex with the S peptide, RNase S (T_M of 48 °C). The results from mixing calorimetry were complicated due to the low T_0 of the S protein (i.e., at temperatures above ca. 15 °C, mixing of the protein and peptide resulted in heat effects from refolding as well as from binding), but results at lower temperature may be used to estimate a $\Delta H_L(T_0)$ of −45 kcal and ΔC_{pL} of −700 cal/deg. With these as fixed parameters in simulations (case I), a T_M of 48 °C at the DSC concentrations ($P_t = L_t = 0.4$ mM) requires a K_L(35 °C) value of 5×10^6 M^{-1}. Extrapolation to 5 °C (using the heat and heat capacity of binding given above) leads to K_L(5 °C) of 2×10^9 M^{-1}, which is in excellent agreement with the value (2.9×10^9 M^{-1}) that Hearns et al. obtained at the same temperature and in the same solvent system. Their estimate was made from measurements of substrate turnover, taking advantage of the fact that the complex is fully active while the S protein itself has no activity.

Trypsin–Soybean Trypsin Inhibitor (STI), Trypsin–Chicken Ovomucoid (OM) and Trypsin–Bovine Pancreatic Trypsin Inhibitor (BPTI). Each of these inhibitors forms a 1:1 complex with bovine β-trypsin and both the complexed and uncomplexed proteins have been studied (Donovan & Beardslee, 1975e; Zahnley, 1979) at pH 6.7. The studies were carried out with a conventional DSC, rather than ultrasensitive, so that concentrations were large, scan rates high, and ΔC_p effects were not estimated (although they appear to be small). Even though these systems showed little or no reversibility on second heatings (as is also typical of some of the other systems discussed below), convincing arguments have been made by Sturtevant and colleagues (Sturtevant, 1987; Manly et al., 1985; Edge et al., 1985, 1988; Hu & Sturtevant, 1987) to suggest that the application of thermodynamic models to such systems is appropriate in many cases, and we will proceed with this assumption.

By use of the intrinsic transition parameters for each of the isolated proteins [trypsin, T_0 of 72.3 °C, $\Delta H(T_0)$ of 194 kcal; STI, T_0 of 76.3 °C, $\Delta H(T_0)$ of 110 kcal; OM, T_0 of 79.0 °C, $\Delta H(T_0)$ of 152 kcal; BPTI, since its T_0 of 103 °C is about the same as or slightly higher than that of the trypsin–BPTI complex, its intrinsic transition parameters are not involved in calculation of K_L], the T_M values for the complexes at 1:1 molar ratios (trypsin–STI, 88.3 °C; Trypsin–OM, 82.5 °C; trypsin–BPTI, 101 °C), and the heats and heat capacities of binding (Baugh & Trowbridge, 1972) from mixing calorimetry [trypsin–STI, $\Delta H_L = 8600 - 442\ (t - 25)$ cal; trypsin–OM, $\Delta H_L = 5595 - 270(t - 25)$ cal; trypsin–BPTI, no information is available from mixing calorimetry], the corresponding K_L values may be estimated at T_0 from simulations and corrected to 25 °C by using the heats and heat capacities of binding where available. For the first two of these complexes, the T_M's are higher than the T_0 of either of the components in the complex so that case II simulations (see Figure 7) must be used.

The value obtained at 25 °C for the trypsin–STI complex from these data is 8×10^{10} M^{-1}, which compares well with a value of ca. 5×10^{10} M^{-1} indicated from the data of Laskowski and Finkenstadt (1972) at similar pH and temperature. For the trypsin–OM complex, the DSC estimate is 2.5×10^7 M^{-1}, which is also close to the literature estimate of 3.2×10^7 M^{-1} (Laskowski & Sealock, 1971) at the same temperature and nearly the same pH. For both complexes, the literature estimates were arrived at from careful studies of proton release upon complex formation using a highly sensitive vibrating reed electrometer. Since no information is available on the heat or heat capacity of binding BPTI to trypsin, it was assumed to be the same as for the trypsin–STI complex. This lead to a K_L(25 °C) of 2×10^{13} M^{-1}, which is close to the independent estimate at the same temperature and pH 8 (Vincent & Lazdunski, 1972) of 1.6×10^{13} M^{-1}, obtained by using radiolabeled BPTI in competition with other weaker binding inhibitors whose interaction constants were known.

Chymotrypsin–Subtilisin Inhibitor (SSI) and Subtilisin BPN′–SSI. These two complexes have been studied by DSC (Fukada et al., 1985; Takahashi & Sturtevant, 1981) and by mixing calorimetry to determine the heats and heat capacities of binding [see Fukada et al. (1985)] at pH 7.0. The inhibitor SSI exists as a tightly coupled dimer I_2, and both of the enzymes are known to form the two-site complex E_2I_2. For the chymotrypsin case, T_M for the complex (56.5 °C) is between T_0 for chymotrypsin (49 °C) and SSI (81.5 °C) while for subtilisin BPN (T_0 of 68.3 °C), the complex is more stable and its T_M (87.5 °C) is higher than that of either isolated component. In the latter case, at inhibitor/enzyme ratios where one might expect to see transitions for the EI_2 complex, only the transition for the E_2I_2 complex is seen. As discussed earlier (cf. Figure 9A), this may mean that site-exchange kinetics are fast enough for rearrangement of subtilisin to occur as T_0 of SSI is exceeded.

Unlike the case of trypsin–inhibitor complexes discussed above, the DSC estimates (using case II simulations for 1:1 rather 2:1 stoichiometry but expressing the concentration, intrinsic heat, and heat capacity of SSI on a per site basis) of interaction constants at 25 °C (2.5×10^6 M^{-1} for chymotrypsin and 3×10^{14} M^{-1} for subtilisin) appear to be substantially in error [ca. 10 times larger (Inouye et al., 1979) and $10^{3.5}$ times larger (Uehara et al., 1978), respectively]. Although we do not know the reason for this discrepancy, it

could have to do with overestimates in the intrinsic transition heats for chymotrypsin and subtilisin. One problem that is known to occur in DSC studies of proteases is that near T_0 the unfolded form is an excellent substrate for the folded form [Takahashi and Sturtevant (1981); Unpublished observations from our laboratory] so that the apparent ΔH for protease transitions will include all additional heat effects arising from chain cleavage as well as those due to the thermal transition itself. This should be a bigger problem in these studies of the SSI complexes than in the studies of the trypsin complexes since scan rates were 10 times slower. In fact, the ΔH values reported by Fukada et al. (1985) for chymotrypsin are more than 30% larger than those reported for the zymogen (Jackson & Brandts, 1970) at a similar temperature, and those for subtilisin (Takahashi & Sturtevant, 1981) are about twice as large as those found for the same protein in the presence of a small inhibitor of its activity (Pantoliano et al., 1989).

Biotin Binding to Avidin. Avidin is a tetramer with four identical binding sites for biotin. The single-site binding constant is too large to be measured directly at pH 7, but appears to be 10^{15} M^{-1} (25 °C) or larger at pH 5, judging by the ratio of rate constants for association and dissociation (Green, 1963) of the complex. Although it was suggested that the four sites are independent (Green, 1966), the evidence for this (i.e., lack of dependence of the heat of binding on the degree of saturation) is inconclusive. From mixing calorimetry, the heat of binding (25 °C) was found to be −22.5 kcal/mol of sites (Suurkuusk & Wadso, 1972) with a large ΔC_p of −240 cal/deg.

From DSC studies (Donovan & Ross, 1973), avidin by itself was shown to have a T_0 of 85 °C at pH 6.8 with ΔH of 75 kcal/mol of sites and ΔC_p of 3000 cal/deg. At a 1:1 molar ratio of biotin to avidin sites, the transition temperature increased by 48 °C to ca. 133 °C! Since no transitions were reported for species with less than four bound ligands, only the geometric average for the single-site binding constant can be estimated. The value is 1×10^{16} M^{-1} at 85 °C or 4×10^{19} M^{-1} at 25 °C. Although this estimate at pH 6.7 is somewhat larger than the estimate of Green (1963) at pH 5, it was reported (Green, 1966) that binding constants at pH 7 were considerably larger than at pH 5 for weaker binding derivatives of biotin.

Metal Ion Binding to Ovotransferrin, Alkaline Phosphatase, and Superoxide Dismutase. Ovotransferrin has two strong iron binding sites located in separate N- and C-terminal domains (Brock, 1985; Aisen & Listowsky, 1980). The binding is too tight to permit determination of free ferric or ferrous ion, which makes estimates of binding constants very uncertain at the least. The difficulties are compounded as on-times are very short and off-times very long, so that initial binding to sites is kinetically controlled and equilibration to thermodynamic distributions may take months under some conditions. The addition of iron chelators has been used to speed up this process. Various estimates of binding constants range over many orders of magnitude, but recent estimates are often in the 10^{20} M^{-1} range (Brock, 1985) near pH 7. It has been suggested at various times that the sites are identical, nonidentical, independent, cooperative, and anticooperative.

The unfolding of ovotransferrin has been observed by DSC at varying levels of saturation with Fe^{3+} (Donovan et al., 1976; Donovan & Ross, 1975b), using a fast scan rate of 10 °C/min. In the absence of metal ion, only a single transition was seen (T_0 of 63 °C). At Fe^{3+} concentrations corresponding to 50% saturation of sites, four transitions were seen and these were assigned to the unliganded (63 °C), two singly liganded (68 and 76 °C), and a doubly liganded (84 °C) species. If these assignments are correct,[3] this system then must be in a frozen state (cf. Figure 9B), in keeping with the very slow ligand exchange and the fast scan rate in these studies.[4] By using the reported transition parameters (ΔH of 320 kcal/mol, ΔC_p of 12000 cal/deg·mol) and an assumed heat of binding of −20 kcal/mol/site, intrinsic binding constants can be estimated (63 °C) as $K_{L1} = 2 \times 10^{13}$ and $K_{L2} = 2 \times 10^7$ M^{-1} with a large cooperativity factor k of 10^5 (i.e., $kK_{L1}K_{L2} = 4 \times 10^{25}$), using calculations from case III in the Appendix. In spite of this large positive cooperativity, the second ligand will still bind somewhat weaker (i.e., $kK_{L2} = 2 \times 10^{12}$) than the first ($2 \times 10^{13}$) during thermodynamic saturation, which means the system would appear to show negative cooperativity if the common assumption were made that intrinsic binding constants for the two sites were nearly identical.

The binding of Zn^{2+} ions to the apoenzymes of both alkaline phosphatase (Chlebowski & Mabrey, 1977) and superoxide dismutase (Roe et al., 1988) has been studied by DSC. Each protein contains two identical subunits and two sites that bind Zn^{2+} very tightly. At zinc ion to protein ratios far smaller than 2.0, DSC peaks are seen only for the apoenzyme and the enzyme with two attached zinc ions, which is quite different from the situation with ovotransferrin discussed above. These observations led both groups of authors to conclude that the binding of the two zincs to the native apoenzyme was cooperative, which accounted for their failure to observe the singly liganded species. Although this could be the correct explanation, it seems at least equally likely that ligand rearrangement might have occurred during the scan that would act to unpopulate the singly liganded form.

The geometric mean for the single-site binding constant $(kK_{L1}K_{L2})^{1/2}$, from these DSC data is ca. 10^{17} M^{-1} for alkaline phosphatase (pH 7.5, 57 °C) and 10^8 M^{-1} for superoxide dimutase (pH 5.5, 57 °C). Although there is no literature estimate for the binding constant of zinc to superoxide dismutase, it is interesting to examine literature data on zinc binding to alkaline phosphatase. Coleman et al. (1983) studied this process by equilibrium dialysis using $^{65}Zn^{2+}$. When equilibrium was approached by using less than saturating concentrations of zinc with the apoenzyme, they found binding constants of 10^5–10^7 M^{-1} for the two tight sites. However, when equilibrium was approached from the other direction by starting with completely saturated enzyme and dialyzing out excess $^{65}Zn^{2+}$ for times up to 10 days, the binding constants were too large to measure ($>10^8$ M^{-1}). This failure to reach

[3] Although we will proceed under the assumption that these literature assignments are correct, there is a different interpretation not considered by the above authors that we feel to be an attractive alternative. For a two-domain protein showing only a single unfolding transition, such as ovotransferrin, it has been shown (Brandts et al., 1989) that tight binding of a ligand to one domain will produce thermodynamic effects that push toward uncoupling into two separate transitions. If this were the case, then the peak at 68 °C would be for the unliganded single domain and that at 76 °C for the liganded single domain, and interpretation of the data would lead to quite different estimates of interaction constants.

[4] If the values for K_{L1}, K_{L2}, and $kK_{L1}K_{L2}$ estimated here are correct then, at 50% saturation of sites, the low-temperature equilibrium distribution would consist of ca. 20% unliganded, 20% doubly liganded, 60% singly liganded (K_{L1}), and 0% singly liganded (K_{L2}) forms. Rearrangements during equilibrium scanning would lead to 50% of the protein participating in the transition for the unliganded form and 50% in the transition of the doubly liganded form. Comparing this to actual DSC results, which show sizable transitions for all four forms, suggests two conclusions. First, the low-temperature distribution that exists probably results from kinetic entrapment during titration, know to occur often for ovotransferrin. Second, this low-temperature distribution remains frozen during scanning.

the same equilibrium from the forward and reverse directions shows that kinetic barriers limited the ability to obtain a true binding constant. Csopak (1969) had earlier used the same techniques as Coleman et al. except for the inclusion of a competing chelator, 1,10-phenanthroline, in the buffer. His estimate of the binding constant (10^{11} M^{-1} at 25 °C, pH 7.5) approaching from the low-ligand direction was substantially larger than that of Coleman et al., perhaps due to the expected effect of the chelator in suppressing kinetic barriers. Since the DSC estimate is orders of magnitude larger yet, this might mean that it approaches closer to the true equilibrium situation. It is reasonable that this could happen, since kinetic barriers might be largely abolished near T_M where molecules will be oscillating quickly between folded and unfolded states.

Assembly of Native Aspartate Transcarbamoylase. It has not yet been possible by any modification of equilibrium methods to characterize the assembly of native ATCase from the regulatory dimers and catalytic trimers, which occurs according to the reaction: $3r_2 + 2c_3 = c_6r_6$. By use of the DSC data of Edge et al. (1988) and the mixing calorimetry data of McCarthy and Allewell (1983), the equilibrium constant for the above assembly reaction can be calculated (case IV in the Appendix) as 5×10^{37} at 25 °C and pH 7. To estimate this interaction constant with an equilibrium technique would require an analytical method capable of distinguishing between free and complexed subunits when the total ATCase concentration is ca. 10^{-10} M.

Summary

Results obtained on the binding of 2′CMP to RNase show that it is possible to obtain very accurate binding constants by the DSC method for a well-defined protein–ligand system if the stoichiometry is known. Consistent results were obtained at low RNase concentration, where the binding constant was estimated from changes in T_M with ligand concentration, and at high RNase concentration, where estimates were made from the change in shape of the transition profile under ligand-limited conditions. The behavior of the system was in all cases in agreement with expectations based on simulations. On the other hand, it was shown that binding constants obtained by calculations using derived equations, of the type used occasionally in the past (Schellman, 1975; Crothers, 1971), can be appreciably in error when site saturation is incomplete. This is due to an inability to accurately determine the temperature where folded and unfolded molecules are present in equal amounts, since this can be different from the temperature where half of the total heat change has occurred.

Simulations were also presented and equations derived for two different types of systems that involve two unfolding transitions rather than one. The first of these applies to protein–macromolecule reactions, where the interaction constants may be obtained from DSC results on the isolated components and on the complex between the two components. This treatment was applied to literature DSC data on a number of protease–protease inhibitor complexes and to the self-assembly of ATCase from the catalytic and regulatory subunits. The second involves the characterization of ligand binding to a protein with two interacting domains, where the transition of each domain can be separately resolved in DSC measurements. In this case, one may estimate the enhancement in the binding constant that is due to ligand-dependent changes in domain–domain interactions. This treatment has been applied to the binding of MgATP to phosphoglycerate kinase and the binding of MgADP to creatine kinase (Brandts et al., 1989). In each case it was found that ligand binding is enhanced because of more favorable interactions that occur between the two domains as a result of ligand binding.

In the case of a protein that has two binding sites for the same ligand within a single cooperative unit, simulations show that ligand rearrangement will occur spontaneously during a DSC scan as the transition temperature of the unliganded protein is approached. The strong tendency is to form more doubly liganded species and fewer singly liganded species than are present at lower temperatures. The reason this occurs is because free energy must be expended to prevent the protein from unfolding above T_0 and the way to minimize the cost in free energy is to utilize all the binding sites on each "protected" molecule. Some rearrangement of ligands will always occur, except in those cases where ligand-exchange times are too slow to allow it, and then the low-temperature distribution of ligands will be frozen or partially frozen throughout the DSC scan. Of the systems of this type that were discussed, three appeared to involve ligand rearrangement during scanning (i.e., Zn^{2+} with alkaline phosphatase, Zn^{2+} with superoxide dismutase, and subtilisin with subtilisin inhibitor) while one (Fe^{3+} with ovotransferrin) was possibly in a frozen configuration.

For the systems examined in this study, apparent single-site interaction constants (25 °C) ranged from 10^5 (RNase–2′CMP at high salt) to ca. 10^{20} M^{-1} (biotin–avidin), while the interaction constant for assembly of ATCase was estimated at 10^{37} in molarity units. For most of the systems, the DSC estimate of interaction constant compared quite favorably with existing literature estimates, for some it did not for reasons unknown, while for still others this represented the first estimate.

Simulations suggest that single-site interaction constants of 10^{40} M^{-1} or larger can be estimated by DSC methods, and this goes well beyond the range that is accessible to equilibrium methods. In addition, equilibrium studies of ultratight binding are frequently hampered be very slow ligand exchange times from the native protein, or slow conformational changes. This can make it difficult to achieve true equilibrium and lead to underestimates of the binding constant, as seen in literature studies of zinc binding to alkaline phosphatase. It is known (e.g., deuterium-exchange studies) that kinetic barriers of this type are often eliminated by taking the system closer to its thermal transition temperature where both ligand and structure exchange can occur through the unfolded form. In such cases, DSC might be a method of choice even when alternatives exist. However, further studies are needed to establish quantitative reliability. The method should prove most accurate when studying the relative binding affinities of a related set of ligands with the same protein, since all transition parameters used in the simulations or calculations will be the same for each ligand, except the T_M for the complex that can be measured very accurately.

Acknowledgments

We thank Michael Brandts for his help in writing the software for DSC simulations.

Appendix

The derivations below all include the following common *assumptions*: (1) All transitions are two-state. (2) Ligand will bind only to the folded form. (3) All ΔC_p values are temperature-independent. (4) All activity coefficients are unity.

The *abbreviations* to be used include the following: T_0 is the transition midpoint (i.e., equal concentrations of folded and unfolded forms) in the absence of ligand and T_M is the same in the presence of ligand. L_t and P_t are bulk concentrations of ligand and protein, respectively. $\Delta H(T)$ and $K(T)$ correspond to enthalpy change and equilibrium constant for

a reaction at temperature T. The prime designation signifies an unfolded state (i.e., P′ is the unfolded form of P). $K_{eq}(T_M)$ is the equilibrium constant for the unfolding process which is being monitored by DSC at the transition midpoint in question.

The transposition of any equilibrium constant from one temperature T_1 to another temperature T_2 will be carried out frequently by using the equation

$$K(T_2) = K(T_1) \exp\left[-\int_{T_1}^{T_2} \Delta H(T)/R \, d(1/T)\right] \quad (1)$$

Expressing $\Delta H(T)$ as either $\Delta H(T_1) + \Delta C_p(T - T_1)$ or as $\Delta H(T_2) + \Delta C_p(T - T_2)$ leads to the following pair of equivalent equations:

$$K(T_2) = K(T_1) \exp[-\Delta H(T_2)/R(1/T_2 - 1/T_1) + \Delta C_p/R(\ln T_2/T_1 + 1 - T_2/T_1)] \quad (2)$$

$$K(T_2) = K(T_1) \exp[-\Delta H(T_1)/R(1/T_2 - 1/T_1) + \Delta C_p/R(\ln T_2/T_1 + T_1/T_2 - 1)] \quad (3)$$

In the following, five different types of interacting systems will be considered. Frequently, binding parameters may be obtained from DSC data either from *calculations* using discrete equations or by fitting the experimental data using *simulations*. For most of the cases to be considered, both of these methods will be treated.

I. Binding Stoichiometry 1:1: Single Unfolding Transition

reactions		parameter set
P = P′	$K = [P']/[P]$	T_0, $\Delta H(T_0)$, ΔC_p
P + L = PL	$K_L = [PL]/[P][L]$	$K(T_0)$, $\Delta H_L(T_0)$, ΔC_{pL}

Calculations:

$$K_{eq}(T) = \frac{[\text{unfolded}]}{[\text{folded}]} = \frac{[P']}{[P] + [PL]} = \frac{K(T)}{1 + K_L(T)[L]} \quad (4)$$

$$K_{eq}(T_M) = 1 = K(T_M)/[1 + K_L(T_M)[L]_{T_M}] \quad (5)$$

where $[L]_{T_M}$ is free ligand concentration at T_M. Since $K(T_0) = 1$, then

$$K_L(T_M) = [\exp[-\Delta H(T_0)/R(1/T_M - 1/T_0) + \Delta C_p/R(\ln T_M/T_0 + T_0/T_M - 1)] - 1]/[L]_{T_M} \quad (6)$$

When both liganded and unliganded molecules are participating in the transition it becomes very difficult to determine T_M and therefore to apply eq 6 as explained in the text. We will therefore restrict the use of eq 6 to tight-binding conditions where T_M can be determined readily and under these conditions the exponential term in the numerator is much larger than unity, so that

$$K_L(T_M) = \exp[-\Delta H(T_0)/R(1/T_M - 1/T_0) + \Delta C_p/R(\ln T_M/T_0 + T_0/T_M - 1)]/[L]_{T_M} \quad (7)$$

where

$$[L]_{T_M} = L_t/2 \text{ if } L_t \le P_t \text{ and } [L]_{T_M} = L_t - P_t/2 \text{ if } L_t \ge P_t \quad (8)$$

If the heat and heat capacity of binding are known from mixing calorimetry, then $K_L(T)$ may be obtained from $K_L(T_M)$ according to

$$K_L(T) = K_L(T_M) \exp[-\Delta H_L(T)/R(1/T - 1/T_M) + \Delta C_{pL}/R(\ln T/T_M + 1 - T/T_M)] \quad (9)$$

If mixing calorimetry data are not available, then the heat of binding may sometimes be estimated from the DSC heat, ΔH_{exp}, using the following equation:

$$\Delta H_{exp}(T_M) = \Delta H(T_0) + \Delta C_p(T_M - T_0) - [K_L[L]/(1 + K_L[L])]\Delta H_L \quad (10)$$

where the multiplier of ΔH_L is the fraction of protein that is liganded at some temperature immediately before the onset of the transition or may be set equal to unity when saturation is complete. DSC data will almost never be precise enough to estimate ΔC_{pL}, but approximate values of $K_L(T)$ may be obtained with only the first-exponential term in eq 9, using ΔH_L from eq 10.

Simulations. The equations for the conservation of mass

$$P_t = [P] + [P'] + [PL] = [P] + K[P] + K_L[L][P] \quad (11)$$

$$L_t = [L] + [PL] = [L] + K_L[L][P] \quad (12)$$

may be solved to obtain concentration of species

$$[L] = \frac{-b + (b^2 - 4ac)^{1/2}}{2a} \quad (13)$$

where $a = K_L$, $b = 1 + K + K_L(P_t - L_t)$, and $c = -L_t(1 + K)$

$$[P] = P_t/(1 + K + K_L[L]) \quad (14)$$

$$[PL] = K_L[P][L] \quad (15)$$

If the input parameters T_0, $\Delta H(T_0)$, ΔC_p, $K_L(T_0)$, $\Delta H_L(T_0)$, ΔC_{pL}, P_t, and L_t are known, then the concentration of all species may be determined at any temperature from eqs 13–15 and the following equilibrium constants:

$$K(T) = \exp[-\Delta H(T_0)/R(1/T - 1/T_0) + \Delta C_p/R(\ln T/T_0 + T_0/T - 1)] \quad (16)$$

$$K_L(T) = K_L(T_0) \exp[-\Delta H_L(T_0)/R(1/T - 1/T_0) + \Delta C_{pL}/R(\ln T/T_0 + T_0/T - 1)] \quad (17)$$

whereupon the excess enthalpy (relative to zero for P species at each temperature) will be

$$\bar{H}_{xs}(T) = [P']/P_t[\Delta H(T_0) + \Delta C_p(T - T_0)] + [PL]/P_t[\Delta H_L(T_0) + \Delta C_{pL}(T - T_0)] \quad (18)$$

The DSC parameter $\bar{C}_{p_{xs}}(T)$ may then be obtained from $\bar{H}_{xs}(T)$ by numerical differentiation over small temperature intervals.

II. Binding Stoichiometry 1:1: Two Unfolding Transitions

This is very similar to case I above, except the "ligand" also has an unfolding transition, with midpoint T_0', so the treatment is applicable to macromolecule–macromolecule interactions. It will be assumed here that T_M for the complex is higher than both T_0 and T_0' since, if this is not true, case I is appropriate.

reactions		parameter set
P = P′	$K = [P']/[P]$	T_0, $\Delta H(T_0)$, ΔC_p
L = L′	$K' = [L']/[L]$	T_0', $\Delta H'(T_0')$, $\Delta C_p'$
P + L = PL	$K_L = [PL]/[P][L]$	$K_L(T_0)$, $\Delta H_L(T_0)$, ΔC_{pL}

Calculations:

$$K_{eq}(T_M) = [P'][L']/[PL] = K(T_M)K'(T_M)/K_L(T_M) \quad (19)$$

$$K_L(T_M) = K(T_M)K'(T_M)/K_{eq}(T_M) \quad (20)$$

Under strong binding conditions

$$K_{eq}(T_M) = L_t - P_t/2 \text{ if } L_t \ge P_t \text{ and } P_t - L_t/2 \text{ if } L_t \le P_t \quad (21)$$

Extrapolating K from T_0 to T_M and K' from T_0' to T_M then gives

$$K_L(T_M) = 1/K_{eq}(T_M) \exp[-\Delta H(T_0)/R(1/T_M - 1/T_0) + \Delta C_p/R(\ln T_M/T_0 + T_0/T_M - 1) - \Delta H'(T_0')/R(1/T_M - 1/T_0') + \Delta C_p'/R(\ln T_M/T_0' + T_0'/T_M - 1)] \quad (22)$$

Once $K_L(T_M)$ is obtained it may be extrapolated to any other

temperature T if the heat and heat capacity of binding are known, i.e.

$$K_L(T) = K_L(T_M)\exp[-\Delta H_L(T)/R(1/T - 1/T_M) + \Delta C_{pL}/R(\ln T/T_M + 1 - T/T_M)] \quad (23)$$

Simulations. Equations for the conservation of mass are

$$P_t = [P] + [P'] + [PL] = [P] + K[P] + K_L[P][L] \quad (24)$$

$$L_t = [L] + [L'] + [PL] = [L] + K'[L] + K_L[P][L] \quad (25)$$

Expressions for species concentrations may be obtained by solving the mass equations

$$[P] = \frac{-b + (b^2 - 4ac)^{1/2}}{2a} \quad (26)$$

where $a = K_L + KK_L$, $b = 1 + K + K' + KK' + K_L(L_t - P_t)$, and $c = -P_t(1 + K')$.

$$[L] = L_t/(1 + K' + K_L[P]) \quad (27)$$

$$[P'] = K[P] \quad (28)$$

$$[L'] = K'[L] \quad (29)$$

$$[PL] = K_L[P][L] \quad (30)$$

Using eqs 26–30 and the following expressions for equilibrium constants

$$K_L(T) = K_L(T_0)\exp[-\Delta H_L(T_0)/R(1/T - 1/T_0) + \Delta C_{pL}/R(\ln T/T_0 + T_0/T - 1)] \quad (31)$$

$$K(T) = \exp[-\Delta H(T_0)/R(1/T - 1/T_0) + \Delta C_p/R(\ln T/T_0 + T_0/T - 1)] \quad (32)$$

$$K'(T) = \exp[-\Delta H'(T_0')/R(1/T - 1/T_0') + \Delta C_p'/R(\ln T/T_0' + T_0'/T - 1)] \quad (33)$$

leads to numerical estimates of all species concentrations at any temperature T, and then the excess enthalpy function may be obtained as

$$\bar{H}_{xs}(T) = [P']/P_t[\Delta H(T_0) + \Delta C_p(T - T_0)] + [L']/P_t[\Delta H'(T_0') + \Delta C_p'(T - T_0')] + [PL]/P_t[\Delta H_L(T_0) + \Delta C_{pL}(T - T_0)] \quad (34)$$

from which the excess heat capacity may be calculated numerically.

III. Binding Stoichiometry 2:1: Single Unfolding Transition

reactions		parameter set
P = P′	$K = [P']/[P]$	T_0, $\Delta H(T_0)$, ΔC_p
P + L = PL	$K_{L1} = [PL]/[P][L]$	$K_{L1}(T_0)$, $\Delta H_{L1}(T_0)$, ΔC_{pL1}
P + L = LP	$K_{L2} = [LP]/[P][L]$	$K_{L2}(T_0)$, $\Delta H_{L2}(T_0)$, ΔC_{PL2}
P + 2L = LPL	$kK_{L1}K_{L2} = [LPL]/[P][L]^2$	k, $\Delta H_{L1}(T_0) + \Delta H_{L2}(T_0)$, $\Delta C_{pL1} + \Delta C_{pL2}$

Calculations. Under certain ligand-limiting conditions (see text) it is possible that up to four transitions may be seen for this system, corresponding to the unliganded (T_0), the two singly liganded (T_{M1} and T_{M2}), and the doubly liganded complex (T_{M12}) with $T_0 < T_{M1} < T_{M2} < T_{M12}$. The following equations apply for the transitions of the three complexes at T_{M1}, T_{M2}, and T_{M12}.

$$K_{eq}(T_{M1}) = \frac{[P'][L]}{[PL]} = \frac{K(T_{M1})}{K_{L1}(T_{M1})} \quad (35)$$

$$K_{L1}(T_{M1}) = \exp[-\Delta H(T_0)/R(1/T_{M1} - 1/T_0) + \Delta C_p/R(\ln T_{M1}/T_0 + T_0/T_{M1} - 1)]/K_{eq}(T_{M1}) \quad (36)$$

$$K_{eq}(T_{M2}) = \frac{[P'][L]}{[LP]} = \frac{K(T_{M2})}{K_{L2}(T_{M2})} \quad (37)$$

$$K_{L2}(T_{M2}) = \exp[-\Delta H(T_0)/R(1/T_{M2} - 1/T_0) + \Delta C_p/R(\ln T_{M2}/T_0 + T_0/T_{M2} - 1)]/K_{eq}(T_{M2}) \quad (38)$$

$$K_{eq}(T_{M12}) = \frac{[P'][L]^2}{[LPL]} = \frac{K(T_{M12})}{kK_{L1}(T_{M12})K_{L2}(T_{M12})} \quad (39)$$

$$kK_{L1}(T_{M12})K_{L2}(T_{M12}) = \exp[-\Delta H(T_0)/R(1/T_{M12} - 1/T_0) + \Delta C_p/R(\ln T_{M12}/T_0 + T_0/T_{M12} - 1)]/K_{eq}(T_{M12}) \quad (40)$$

Before evaluating K_{eq} at each T_M, an estimate must be made for the amount of protein participating in each of the four transitions (i.e., from the areas under each peak after adjusting for the heat capacity effect and heat of binding, if known). Once these quantities are known, each K_{eq} may be evaluated (e.g., at T_{M12}, [P′] will be equal to the sum of concentrations of all protein involved in the first three transitions plus half of that in the fourth transition, etc.). Once equilibrium constants are obtained at each T_M, they may be extrapolated to other temperatures if the heats and heat capacities of binding are known, as illustrated earlier.

Simulations. The equations for the conservation of mass are

$$P_t = [P] + K[P] + K_{L1}[P][L] + K_{L2}[P][L] + kK_{L1}K_{L2}[P][L]^2 \quad (41)$$

$$L_t = [L] + K_{L1}[L][P] + K_{L2}[L][P] + 2kK_{L1}K_{L2}[P][L]^2 \quad (42)$$

Combination of these two simultaneous equations leads to a cubic equation in [L]. There are two pertinent roots for [L], depending on input parameters and temperature. Only one of these will lie between 0 and L_t. The expressions for these roots are

$$[L] = -p/3 + [-b/2 + (b^2/4 + a^3/27)^{1/2}]^{1/3} + [-b/2 - (b^2/4 + a^3/27)^{1/2}]^{1/3} \quad (43)$$

and

$$[L] = -p/3 + 2(-a/3)^{1/2}\cos X/3 \quad (44)$$

where

$$\cos X = -b/2(-a^3/27)^{-1/2}$$

$$p = K_{L1} + K_{L2} + kK_{L1}K_{L2}(2P_t - L_t)$$

$$q = [1 + K + (K_{L1} + K_{L2})(P_t - L_t)]/[kK_{L1}K_{L2}]$$

$$r = -L_t(1 + K)/[kK_{L1}K_{L2}]$$

$$a = (3q - p^2)/3$$

$$b = (2p^3 - 9pq + 27r)/27$$

By use of the temperature-dependent expressions for K, K_{L1}, and K_{L2} in the same way as in cases I and II, [L] may be calculated and then [P], [P′], [PL], [LP], and [LPL] by using eq 42 and appropriate equilibrium constants.

The excess enthalpy function for this system will be

$$\bar{H}_{xs}(T) = ([PL] + [LPL])/P_t[\Delta H_{L1}(T_0) + \Delta C_{pL1}(T - T_0)] + ([LP] + [LPL])/P_t[\Delta H_{L2}(T_0) + \Delta C_{pL2}(T - T_0)] + [P']/P_t[\Delta H(T_0) + \Delta C_p(T - T_0)] \quad (45)$$

This assumes that the site–site interaction term k does not have appreciable enthalpy associated with it. The excess heat ca-

pacity $\bar{C}_{p_{xs}}$ may then be obtained as described earlier.

IV. General i:n Stoichiometry: One or Two Unfolding Transitions

reactions		parameter set
R = R′	$K = [R']/[R]$	T_0, $\Delta H(T_0)$, ΔC_p
C = C′	$K' = [C']/[C]$	T_0', $\Delta H'(T_0')$, $\Delta C_p'$
$iR + nC = R_iC_n$	$K_L = [R_iC_n]/([R]^i[C]^n)$	$K_L(T_0)$, $\Delta H_L(T_0)$, ΔC_{pL}

Calculations. This treatment is intended for subunits that assemble in one cooperative step into a complex R_iC_n, such as occurs for ATCase. The transition temperature for unfolding of the complex, T_M, may occur either between the intrinsic transition temperatures T_0 and T_0' for the isolated subunits or at a temperature above both T_0 and T_0'. It will be assumed for the moment that T_M is higher than both T_0 and T_0'; we will later indicate the changes that must be made if this is not the case. It will also be assumed for simplicity that the subunits are present in stoichiometric equivalent amounts so that the only concentration that need to be considered is the bulk molar concentration of the complex, which is designated P_t.

$$K_{eq}(T_M) = [R']^i[C']^n/[R_iC_n] = (i)^i(n)^n(P_t/2)^{i+n-1} = K(T_M)^iK'(T_M)^n/K_L(T_M) \quad (46)$$

$$K_L(T_M) = \exp[-i\Delta H(T_0)/R(1/T_M - 1/T_0) + i\Delta C_p/R(\ln T_M/T_0 + T_0/T_M - 1) - n\Delta H'(T_0')/R(1/T_M - 1/T_0') + n\Delta C_p'/R(\ln T_M/T_0' + T_0'/T_M - 1)]1/[(i)^i(n)^n(P_t/2)^{i+n-1}] \quad (47)$$

If it happens that T_M occurs above T_0 but below T_0', then eq 47 will still be valid if the two terms involving $\Delta H'(T_0)$ and $\Delta C_p'$ are omitted in the exponential function. Once K_L at T_M is obtained, extrapolation to other temperatures may be carried out as before if the heat and heat capacity for the assembly reaction are known.

Simulations. Once the sum of $(i + n)$ exceeds 3, then the conservation of mass equations are more readily solved by iterative, numerical methods, rather than in closed form.

V. Binding of 1:1 Stoichiometry to a Two-Domain, Two-Transition Protein

reactions		parameter set
AB = A′B	$K_A = [A'B]/[AB]$	T_{0A}, $\Delta H_A(T_{0A})$, ΔC_{pA}
A′B = A′B′	$K_B = [A'B']/[A'B]$	T_{0B}, $\Delta H_B(T_{0B})$, ΔC_{pB}
A′B + L = A′BL	$K_L = [A'BL]/([A'B][L])$	$K_L(T_{0A})$, $\Delta H_L(T_{0A})$, ΔC_{pL}
AB + L = ABL	$kK_L = [ABL]/([AB][L])$	$kK_L(T_{0A})$, $\Delta H_L(T_{0A})$ + $\Delta(\Delta H)$, ΔC_{pL}

It is assumed here that A and B are two interacting domains and that interactions between the two domains change when a ligand L binds to the B domain (Brandts et al., 1989) in the native AB state. The unfolding transition for the regulatory A domain is at T_{0A} in the absence of ligand, which is assumed to be lower than T_{0B} for the binding domain. Since all interactions between domains are assumed to disappear if either of the two domains is unfolded, then the enhancement factor k [with its associated $\Delta(\Delta H)$] will be greater than unity if ligand binding increases A···B interactions and smaller than unity if it reduces interactions. Since equations were derived earlier (Brandts et al., 1989) for calculating binding parameters for this sytem, only the simulations will be treated here.

The equations for the conservation of mass are

$$P_t = [AB][1 + K_A + K_AK_B + K_AK_L[L] + kK_L[L]] \quad (48)$$

$$L_t = [L][1 + kK_L[AB] + K_AK_L[AB]] \quad (49)$$

These may be solved to obtained the free ligand concentration

$$[L] = \frac{-b + (b^2 - 4ac)^{1/2}}{2a} \quad (50)$$

where $a = K_LK_A + kK_L$, $b = 1 + K_A + K_AK_B + (kK_L + K_AK_L)(P_t - L_t)$, and $c = -L_t(1 + K_A + K_AK_B)$. Then [AB] may be determined from eq 48 and all other species concentrations are available from the equilibrium constants. The excess enthalpy function is

$$\bar{H}_{xs}(T) = ([A'B]/P_t)[\Delta H_A(T_{0A}) + \Delta C_{pA}(T - T_{0A})] + ([A'B']/P_t)[\Delta H_A(T_{0A}) + \Delta H_B(T_{0B}) + \Delta C_{pA}(T - T_{0A}) + \Delta C_{pB}(T - T_{0B})] + ([ABL]/P_t)[\Delta H_L(T_{0A}) + \Delta(\Delta H) + \Delta C_{pL}(T - T_{0A})] + ([A'BL]/P_t)[\Delta H_A(T_{0A}) + \Delta H_L(T_{0A}) + (\Delta C_{pA} + \Delta C_{pL})(T - T_{0A})] \quad (51)$$

and the excess heat capacity can be obtained by numerical differentiation.

Registry No. CMP, 85-94-9; RNase, 9001-99-4; RNase S peptide, 65742-22-5; Fe, 7439-89-6; Zn, 7440-66-6; trypsin, 9002-07-7; soybean trypsin inhibitor, 9078-38-0; basic pancreatic trypsin inhibitor, 9087-70-1; chymotrypsin, 9004-07-3; subtilisin, 9014-01-1; biotin, 58-85-5; superoxide dismutase, 9054-89-1; alkaline phosphatase, 9001-78-9; aspartate transcarbamoylase, 9012-49-1.

References

Aisen, P., & Listowsky, I. (1980) *Annu. Rev. Biochem. 49*, 357–393.

Anderson, D. G., Hammes, G. G., & Walz, F. G., Jr. (1968) *Biochemistry 1*, 1637–1645.

Baugh, R. J., & Trowbridge, C. G. (1972) *J. Biol. Chem. 247*, 7498–7501.

Brandts, J. F., Hu, C. Q., Lin, L.-N., & Mas, M. T. (1989) *Biochemistry 28*, 8588–8596.

Brock, J. H. (1985) in *Metalloproteins. Part 2: Metal Proteins with Non-redox Roles* (Harrison, P. M., Ed.) pp 183–219, McMillan, New York.

Chlebowski, J. F., & Mabrey, S. (1977) *J. Biol. Chem. 252*, 7042–7052.

Coleman, J. E., Nakamura, K., & Chlebowski, J. F. (1983) *J. Biol. Chem. 258*, 386–405.

Crothers, D. M. (1971) *Biopolymers 10*, 2147–2160.

Csopak, H. (1969) *Eur. J. Biochem. 7*, 186–192.

Donovan, J. W., & Ross, K. D. (1973) *Biochemistry 12*, 512–517.

Donovan, J. W., & Beardslee, R. A. (1975a) *J. Biol. Chem. 250*, 1966–1971.

Donovan, J. W., & Ross, K. D. (1975b) *J. Biol. Chem. 250*, 6026–6031.

Donovan, J. W., Beardslee, R. A., & Ross, K. D. (1976) *Biochem. J. 153*, 631–639.

Edge, V., Allewell, N. M., & Sturtevant, J. M. (1985) *Biochemistry 24*, 5899–5906.

Edge, V., Allewell, N. M., & Sturtevant, J. M. (1988) *Biochemistry 27*, 8081–8087.

Empie, M. W., & Laskowski, M., Jr. (1982) *Biochemistry 21*, 2274–2284.

Fukada, H., Takahashi, K., & Sturtevant, J. M. (1985) *Biochemistry 24*, 5109–5115.

Garlick, R. K., & Giese, R. W. (1988) *J. Biol. Chem. 263*, 210–215.

Green, N. M. (1963) *Biochem. J. 89*, 599–608.

Green, N. M. (1966) *Biochem. J. 101*, 774–780.

Hearn, R. P., Richards, F. M., Sturtevant, J. M., & Watt, G. D. (1971) *Biochemistry 10*, 806–817.

Hinz, H.-J. (1983) *Annu. Rev. Biophys. Bioeng. 12*, 285–317.

Hu, C. Q., & Sturtevant, J. M. (1987) *Biochemistry 26*, 178–182.

Inouye, K., Tonomura, B., & Hiromi, K. (1979) *J. Biochem. 85*, 601–607.
Jackson, W. M., & Brandts, J. F. (1970) *Biochemistry 9*, 2294–2301.
Laskowski, M., Jr., & Sealock, R. W. (1971) in *The Enzymes* (Boyer, P. D., Ed.) 3rd ed., Vol. 3, pp 375–473, Academic Press, New York.
Laskowski, M., Jr., & Finkenstadt, W. R. (1972) *Methods Enzymol. 26*, 193–227.
Manly, S. P., Matthews, K. S., & Sturtevant, J. M. (1985) *Biochemistry 24*, 3842–3846.
Marky, L. A., & Breslauer, K. J. (1987) *Biopolymers 26*, 1602–1620.
McCarthy, M. P., & Allewell, N. M. (1983) *Proc. Natl. Acad. Sci. U.S.A. 80*, 6824–6828.
Pace, C. N., & McGrath, T. (1980) *J. Biol. Chem. 255*, 3862–3865.
Pantoliano, M. W., Whitlow, M., Wood, J. F., Dodd, S. W., Hardman, K. D., Rollence, M. L., & Bryan, P. N. (1989) *Biochemistry 28*, 7205–7213.
Riggs, A. D., Bourgeois, S., & Cohn, M. (1970) *J. Mol. Biol. 53*, 401–410.
Robert, C. H., Gill, S. J., & Wyman, J. (1988) *Biochemistry 27*, 6829–6835.
Roe, J. A., Butler, A., Scholler, D. M., Valentine, J. S., Marky, L. A., & Breslauer, K. J. (1988) *Biochemistry 27*, 950–958.
Ross, P. D., & Shrake, A. (1988) *J. Biol. Chem. 263*, 11196–11202.
Schellman, J. A. (1975) *Biopolymers 14*, 999–1018.
Schwarz, F. P. (1988) *Biochemistry 27*, 8429–8436.
Shrake, A., & Ross, P. D. (1988) *J. Biol. Chem. 263*, 15392–15399.
Shrake, A., & Ross, P. D. (1990) *J. Biol. Chem.* (in press).
Shrake, A., Finlayson, J. S., & Ross, P. D. (1984) *Vox Sang. 47*, 7–18.
Sturtevant, J. M. (1987) *Annu. Rev. Phys. Chem. 38*, 463–488.
Suurkuusk, J., & Wadso, I. (1972) *Eur. J. Biochem. 28*, 438–442.
Takahashi, K., & Sturtevant, J. M. (1981) *Biochemistry 20*, 6185–6190.
Ts'o, P. O. P., Kondo, N. S., Schweizer, M. P., & Hollis, D. P. (1969) *Biochemistry 8*, 997–1029.
Tsong, T. Y., Hearn, R. P., Wrathall, D. P., & Sturtevant, J. M. (1970) *Biochemistry 9*, 2666–2677.
Uehara, Y., Tonomura, B., & Hiromi, K. (1978) *J. Biochem. 84*, 1195–1202.
Vincent, J.-P., & Lazdunski, M. (1972) *Biochemistry 11*, 2967–2977.
Wiseman, T., Williston, S., Brandts, J. F., & Lin, L.-N. (1989) *Anal. Biochem. 179*, 131–137.
Zahnley, J. C. (1979) *J. Biol. Chem. 254*, 9721–9727.